

SP 61-3

Design Predictions of Crack Widths in Ferrocement

By Antoine E. Naaman

Synopsis: One of the distinguishing features of ferrocement as compared to reinforced concrete is the larger number of finer cracks for the same stresses in the steel reinforcement. Designing ferrocement structures to satisfy recommended serviceability criteria in a manner similar to the design of reinforced concrete structures is a logical and rational approach to follow. Serviceability is greatly dependent on cracking and crack width under working load conditions. Thus the prediction of crack widths (average and/or maximum) is an important consideration in design.

This paper is based on a number of recent investigations on the cracking of ferrocement elements: they include tests on flexural beams under static and fatigue loadings, tests on ferrocement prisms with and without transverse reinforcement subjected to direct tensile loads, and tests on internally pressurized model ferrocement cylindrical water tanks. The following aspects of cracking are clarified for both flexure and tension: cracking behavior; influencing parameters; observed variations of crack widths; crack width predictions and suggested design approach.

Keywords: cracking (fracturing); crack width and spacing; ferrocement; flexural strength; serviceability; structural design; tensile stress; tension tests; wire cloth.

A. E. Naaman is associate professor of structural design, Department of Materials Engineering, University of Illinois at Chicago Circle. Dr. Naaman received his Ph.D. degree from the Massachusetts Institute of Technology in 1972 and is a member of technical committees of ACI, PCI and ASCE.

INTRODUCTION

One of the distinguishing features of ferrocement as compared to reinforced concrete is the larger number of finer cracks for the same stresses in the steel reinforcement. The development of fine cracks under loading makes it possible to build safe ferrocement structures in thin sections and still maintain acceptable appearance, corrosion resistance and virtual watertightness.

Designing ferrocement structures to satisfy recommended serviceability criteria in a manner similar to the design of reinforced concrete structures is a logical and rational approach to follow. Serviceability is greatly dependent on cracking and crack width under working load conditions. Thus the prediction of crack widths (average and/or maximum) is an important consideration in design.

Cracking in reinforced concrete has been the subject of a large number of investigations [1 to 8], which have added to the better understanding of its behavior. Although ferrocement is a type of reinforced concrete--and is expected a priori to behave similarly--its cracking behavior is substantially different [9]. This seems to be due to at least three major differences: 1) ferrocement comes in thin shell-like elements with its reinforcement distributed throughout the section, 2) its specific surface of reinforcement is an order of magnitude higher than that of reinforced concrete (for equal amounts of steel), and 3) the presence of transverse wires in the mesh reinforcement of ferrocement enhances bond transfer properties and cracking characteristics.

As the terms volume fraction and specific surface of reinforcement will be often used in this paper, their meanings are intended as follows: the volume fraction of reinforcement is the ratio of volume of reinforcement per unit volume of composite; it may indicate the total volume V_f or the volume in the loading direction V_{fL} ; note that V_{fL} is quantitatively equal to the reinforcement ratio of the identical reinforced concrete section; the specific surface of reinforcement is the lateral surface (bonded area) of reinforcement per unit volume of composite; it may refer to the total area S_R or to the area in the loading direction S_{RL} . The specific surface and the volume fraction of reinforcement are related by the following relationship:

$$S_R = \frac{4V_f}{\phi} \quad (1)$$

where ϕ is the diameter of the wire used. Note that a similar relationship exists between S_{RL} and V_{fL} .

This paper is based on a number of recent investigations on the cracking of ferrocement elements reinforced mostly with square, galvanized steel meshes; they include tests on flexural beams under static and fatigue loading [10,11,12], tests on prisms subjected to uniaxial tension [13,14] and tests on internally pressurized model ferrocement cylindrical water tanks [15,16]. Based on the observed results, the following aspects of cracking will be clarified for both flexure and tension: cracking behavior; influencing parameters; observed variation of crack widths; crack width prediction and suggested design approach.

UNIAXIAL TENSION

Tensile tests were carried out on prisms which were 12 in. (30 cm) long, 1 in. (2.5 cm) wide and 3/8 in. (\approx 1 cm) thick. The reinforcement consisted of various amounts of either square wire meshes or smooth longitudinal wires (no transverse wires). Only two mesh openings (spacing center-to-center of wires) were tested: 1/4 in. (6.3 mm) and 1/2 in. (12.7 mm). Thus "1/4" or "1/2" will refer to the mesh size or opening. Most of the meshes used were welded meshes and the woven meshes used had a high modulus. The elongation (and equivalently the strain) in the ferrocement composite under load was measured over a 6 in. (15 cm) gage length using a device directly attached to the specimen and equipped with an LVDT. The load-elongation curve was automatically recorded on an electronic XY recorder. Cracks along the observed gage length were detected, counted and their widths measured at different loads using an internally illuminated microscope equipped with a micrometer that allowed an accuracy of about 50 micromin (1.27 x 10⁻³ mm). Details of the above investigation are given in Ref. 14. Only some of the salient remarks and conclusions are described below. They help reinforce some of the findings reported in an earlier investigation on tensile cracking in ferrocement [13] while bringing new and accurate results on crack widths.

1. The tensile stress-strain curve of ferrocement can be generally divided into three stages: a) elastic behavior until the first matrix cracking; b) multiple cracking stage--in this stage the number of cracks keeps increasing with an increase in tensile stress or strain; their width, however, may only slightly increase depending on the reinforcing parameters used, but not in direct proportion to the stress increase; and c) crack widening stage--in this stage no or few additional cracks are formed, the existing cracks become wider and the behavior of the specimen is controlled by that of the reinforcement alone. Typical stress-strain curves of tensile specimens reinforced with longitudinal wires only and with wire meshes are shown in Figs. 1 and 2, respectively.

Figure 1 shows that the number of cracks increases from 1 to 17 while the stress in the longitudinal steel varies from about 20 to 50 ksi (138 to 345 MN/m²); the average crack width, however, increases only slightly from 4×10^{-4} to 5.6×10^{-4} in. (0.010 to 0.014 mm). An identical specimen with smaller number of wires (smaller V_f and S_R) will show a substantially higher increase in crack width for the same stress range. A mixed trend is observed in Fig. 2 for a specimen reinforced with square wire meshes (i.e., having transverse reinforcement); here the number of cracks keeps increasing even in the nonlinear range of behavior of the steel and thus crack width is greatly influenced by the strain increase in the reinforcement. The stress at which the number of cracks stops increasing is termed here the stabilization stress f_{sta} . Depending on the reinforcing parameters, namely specific surface and transverse wire spacing, the stabilization stress may be somewhere along the elastic or nonelastic range of behavior of the steel reinforcement.

2. Everything else being equal, the higher the specific surface and the smaller the transverse wire spacing, the larger the extent of the multiple cracking stage, the larger the number of cracks developed in the same gage length, the smaller the crack spacing and the smaller the crack widths. Thus for specimens having identical longitudinal reinforcement, better cracking characteristics are obtained when transverse reinforcement is used (i.e., meshes versus wires). Figure 3 shows the variations of the number of cracks developed as a function of steel stress for typical tensile specimens with and without transverse reinforcement. A similar curve is also shown for a flexural specimen for comparison.
3. A direct relationship between the average crack spacing $(\Delta l)_{av}$ at crack stabilization and the specific surface of reinforcement seems to exist. An analytical evaluation of this relationship has been proposed in [13] and is given by

$$(\Delta l)_{av} = \frac{\theta}{\eta} \frac{1}{S_{RL}} \quad (2)$$

where $(\Delta l)_{av}$ = average crack spacing

θ = a factor relating average crack spacing to maximum crack spacing

η = ratio of bond strength to matrix tensile strength

S_{RL} = specific surface of reinforcement in the loading direction

As the factor θ/η can be approximated for design purposes a direct relation between $(\Delta l)_{av}$ and S_{RL} can be obtained. The observed values of average crack spacing at crack stabilization

are shown (Fig. 4) versus the specific surface of reinforcement in the loading direction S_{RL} for both the series of specimens reinforced with smooth longitudinal wires and those reinforced with square wire meshes. It can be seen that for the same specific surface, smaller spacings are obtained when the reinforcement contains transverse wires (i.e., meshes). The analytical equation (2) is also plotted with the values of $(\theta/\eta) = 1$ and 2.7. It can be observed that for $(\theta/\eta) = 1$, Eq. (2) predicts very well the experimental data for square meshes while for $(\theta/\eta) = 2.7$ it predicts the data when smooth longitudinal wires are used. Thus Eq. (2) with the above values of the factor θ/η can be used as a design equation to predict crack spacing in ferrocement at crack stabilization.

4. A large number of data on crack widths were generated. They are quite complex to analyze as crack widths depend on many parameters and in ferrocement the extent of the multiple cracking region may have a significant effect on the results. However, as in reinforced concrete the stress in the steel after cracking is of major importance, data on crack widths, average and maximum, were plotted versus the stress in the steel. Typical results are shown in Fig. 5 for one series of tests having six identical specimens. It can be seen that for stresses below 60 to 65 ksi (which are much above recommended design or service stresses), there is little increase in crack width, at least for this series of tests. This is essentially due to the effect of the extent of the multiple cracking stage (which can be visualized in Fig. 2 for one specimen of the above series).
5. The ratio of maximum crack width to average crack width was computed for steel stresses less than 60 ksi, and for all series of tests using square wire meshes. It was generally observed that the higher the specific surface of reinforcement, the smaller the ratio. The mean value of that ratio was equal to 1.85 with a standard deviation of 0.51.
6. For the purpose of design a simple approach to predict maximum crack widths is necessary. A method is proposed here for ferrocement specimens reinforced with square wire meshes. It consists of first predicting a "stabilization stress" f_{sta} and then predicting a maximum crack width value which applies for any stress f_s less than f_{sta} . For stresses above f_{sta} it is expected that the crack width will increase in direct relation to the increase in steel strain; thus it will also directly increase with the steel stress if the latter is less than the yield strength. It will be assumed here that the yield strength will be of the order of 60 ksi. The proposed design approach is summarized as follows:

For $S_{RL} \leq 3 \text{ in.}^{-1}$

- a) Determine stress in the steel at crack stabilization from

$$f_{sta} = 20 S_{RL} \leq 60 \text{ ksi} \quad (3)$$

where f_{sta} is given in ksi for S_{RL} in in.^{-1} .

- b) For any stress less than f_{sta} determine the maximum crack width using

$$W_{max} = \frac{1}{S_{RL}} \frac{f_{sta}}{E_R} = \frac{20}{E_R} \quad (4)$$

where E_R is the modulus of the reinforcing system.

- c) For any stress f_s larger than f_{sta} but less than the yield strength given in ksi use:

$$W_{max} = [6.9 + (f_s - f_{sta})] \frac{29000}{E_R} 10^{-4} \quad (5)$$

where W_{max} is in inches.

For $S_{RL} > 3 \text{ in.}^{-1}$ and for any stress less than the yield strength or about 60 ksi use the following:

$$W_{max} = (15.5 - 3 S_{RL}) 10^{-4} \geq 0.0004 \text{ in.}$$

Figure 6 shows the above relations for various values of S_{RL} and steel stresses.

It is noted that the above proposed approach has provided a reasonable upper bound value to all the data of this investigation. A typical representation of the above equations (3,4,5) is shown in Fig. 5 for the series of tests described in that figure and can be compared to actual values of maximum and average crack widths.

TENSILE CRACKING OF FERROCEMENT WATER TANKS

The detailed information on tests of model ferrocement water tanks has been already published in [15] and [16]. As the crack widths, average and maximum, for the tanks were sometimes higher (up to two or three times) for the same steel stress than those reported above for prisms, a note of clarification is necessary. It is believed that the difference is due to several variables as follows:

- a) The hoop direction of the mesh in the tank was the longitudinal direction of the roll of mesh used, which generally shows a substantially lower modulus than the transverse direction.
- b) The average crack width was calculated as the mean value of only 10 cracks under observation. These cracks (among more than 100 cracks) were detected first and thus had a larger width than the average of all cracks. Thus their average widths is in effect an upper bound measure.
- c) One or two cracks occurred generally in the overlap region of the mesh reinforcement and led to unusually high crack widths, thus substantially influencing, in some instances, the value of maximum and average crack widths.
- d) The ferrocement walls of the water tanks were in effect subject to biaxial tension instead of uniaxial tension. Furthermore, the thickness and reinforcement cover of the walls were not as controlled and constant as in the experiments on prisms.

CRACKING IN FLEXURE

A large number of flexural specimens having overall dimensions of $18 \times 5 \times 1/2$ in. ($457 \times 127 \times 12.7$ mm) were tested, in third point bending, under static and fatigue loads. Details are given in [10,11,12]. The reinforcement consisted of three types of square galvanized steel meshes, $1/2$ woven, $1/2$ welded and $1/4$ woven ($1/2$ and $1/4$ refer to the mesh size or spacing center-to-center of the wires in inches in either direction). For each type of mesh three volume fractions of reinforcement corresponding to 2, 4 and 6 layers of mesh were used. The reinforcing layers were cut along the transverse direction of the mesh rolls to assure a better modulus of the reinforcing system. Generally the layers were stacked in such a way that the transverse wires of the different layers were along the same cross sections. Cracks were measured at different levels of loadings using an internally illuminated microscope fitted with a micrometer that allowed a measuring accuracy of 50 microinch (1.27×10^{-3} mm). The analysis of the data generated by the above investigation leads to a number of pertinent results summarized as follows:

1. The transverse wires of the outermost layer of mesh are preferential locations for cracks. In most specimens the number of cracks in the constant moment zone reached a steady value soon after the occurrence of first cracking (independently of the number of layers used). This steady value corresponds to an average crack spacing equal to the spacing of the transverse wires (Fig. 3).
2. The specific surface of reinforcement did not seem to have as strong an influence on the cracking behavior in flexure as in tension. This may be because in flexure the specific surface in the tensile zone of mortar around the outermost layer of mesh does not increase substantially when the number of mesh layers used increases.

3. A systematic regression analysis of observed crack widths showed that the average crack width is primarily a function of the tensile strain in the extreme layer of mesh and does not depend on the other parameters found important in reinforced concrete. This may be because of the relatively small cover and high specific surface of reinforcement in ferrocement beams.
4. A computerized nonlinear analysis in bending of the ferrocement section showed that the stresses in the mesh reinforcement up to about yielding of the steel can be predicted, with a good approximation, using linear elastic analysis of the cracked section.
5. A linear regression analysis of all the data on crack widths for all the series of tests on static bending leads to the following relationships between crack widths and the stress f_s in the outermost layer of steel mesh:

$$W_{av} = (0.271 f_s - 3.73) 10^{-4} \quad (6)$$

and

$$W_{max} = (0.324 f_s - 4.36) 10^{-4} \quad (7)$$

where W_{av} = average crack width, in.
 W_{max} = maximum crack width, in.
 f_s = stress in the steel in ksi

The above equations as well as the corresponding data are plotted in Figs. 7 and 8. Note that the average secant modulus at 45 ksi of all the meshes used in the above tests was around 23,000 ksi. Note also that each data point of Fig. 7 has a substantial weight as it represents the average reading for at least three specimens, at a given steel stress and for a large number of cracks each of which characterized by two measurements along its length. For example, the data point representing two layers, 1/2 welded at 50 ksi represents the average of about 60 measurements.

A number of linear relationships between crack widths and steel stress, similar to the above, were developed for each type of mesh in Ref. 10 and can be used if a better accuracy is desired.

6. The overall average ratio between maximum crack width and average crack width, for 32 sets of data and for the overall range of steel stress considered, was determined and found equal to 1.21 with a standard deviation of 0.14. It can be observed that the above ratio and the coefficient of variation are substantially smaller than those observed in tensile tests. From the above results it can be concluded that generally the maximum crack width in flexure for ferrocement is, with 98% probability, less than 1.5 times the average crack width.

7. A simple design equation is proposed in Ref. 10 to predict average crack width as a function of steel strain in the outermost layer of mesh. However, when compared to the experimental data the equation gave a useful upperbound value and could be used in effect to predict maximum crack widths. If, in the elastic range of behavior, the stress in the steel is expressed in function of the strain, and W_{\max} is used instead of W_{av} , the prediction equation given in Ref. 10 takes on the following form:

$$W_{\max} = \beta S \frac{f_s}{E_R} \quad (8)$$

where

W_{\max} = maximum crack width, in.

S = mesh size or spacing center-to-center of mesh wires, in inches

β = ratio of distances to the neutral axis from the extreme tensile fiber and from the outermost layer of steel (elastic cracked section analysis)

f_s = steel stress in ksi

E_R = modulus of reinforcing system in ksi

Note that E_R is the same as the modulus of elasticity of the steel for welded meshes but can be substantially lower for woven meshes depending on the pitch of the weave and other parameters. It has been also observed that E_R may be substantially different if measured along the transverse direction instead of the longitudinal direction. For the types of square woven meshes generally used in ferrocement E_R can vary between 15,000 and 29,000 ksi (103,500 to 200,100 MN/m²).

Assuming a value of $\beta = 1.2$, the line corresponding to Eq. (8) is plotted (Fig. 9) for different hypothetical meshes and compared with the regression equations (Eqs. (6) and (7)) from all the data. It can be seen that in view of the variability expected in crack widths, both approaches are acceptable as a design prediction.

Note that the overall average modulus E_R for the flexural experiments described in [10,11] was around 23,000 ksi (158,700 MN/m²). Thus if one can determine the modulus E_R of a given mesh, Eqs. (6) and (7) can be modified to more accurately predict crack widths (given in inches) as follows:

$$W_{\text{av}} = \frac{23000}{E_R} (0.271 f_s - 3.73) 10^{-4} \quad (9)$$

and

$$W_{\max} = \frac{23000}{E_R} (0.324 f_s - 4.36) 10^{-4} \quad (10)$$

for stresses higher than the stress at cracking and smaller than the yield strength and given in ksi.

8. Test results on fatigue loading [12] have indicated that the average and maximum crack width at a given load keep increasing with the number of loading cycles.
9. The following relationship was found [12] acceptable to represent crack width data, average or maximum, under fatigue loading up to about 90% of fatigue life:

$$W = Ae^{Br} \quad (11)$$

where

W = average or maximum crack width

A = value of crack width at maximum load under static test. It could be predicted from Eqs.

e = base of Napierian logarithms

r = cycle ratio; i.e., number of cycles at which crack width is calculated to the number of cycles to failure N_f

B = a parameter determined from the experimental data and described in [12]. A constant value of $B = 1.67$ is proposed for $N_f \geq 450,000$ cycles which is generally the case for most design situations.

In order to use Eq. (11) the number of cycles to failure N_f is needed. A regression analysis of the data [12] between stress range in the steel and the number of cycles to failure has led to the following relation:

$$f_{sr} = 152.3 - 19.5 \log_{10} N_f \quad (12)$$

where

f_{sr} = stress range in the outermost layer of steel in ksi

N_f = number of cycles to failure

Thus if f_{sr} is known, N_f can be predicted, or if a certain value of N_f is required by the design the corresponding limit on stress range can be determined.

A typical example of crack width increase with number of cycles is shown in Fig. 10 curve (a) for a flexural specimen from the tests with the following parameters: 2, 1/2 welded layers of steel mesh (subjected to a fluctuating load of ± 36 lbs; steel

cover = 1/8 in. (3.1 mm)); maximum tensile stress in the steel = 37.81 ksi (261 MN/m²); minimum stress = 1.34 ksi (9.2 MN/m²) (compression); stress range = $f_{sr} = 39.15$ ksi (270 MN/m²); mean stress = 18.23 ksi (126 MN/m²). From Eq. (12), the number of cycles to failure can be estimated as $N_f \approx 635,000$ cycles. The maximum crack width at maximum stress can be predicted for the first cycle from Eq. (7) and leads to $w_{max} = 7.88 \cdot 10^{-4}$ in. (0.020 mm). This gives the value of A of Eq. (11). The maximum crack width at any cycle ratio r can then be calculated from Eq. (11) as $w_{max} = 7.88 e^{1.67r}$ in 10^{-4} in. and is plotted on Fig. 10. Note that Eq. (7) has been used to predict $A = 7.88 \cdot 10^{-4}$. If Eq. (8) was used the result would have been $7.82 \cdot 10^{-4}$. Also on Fig. (10) a number of curves are shown assuming exactly the same specimen subject to the same maximum stress but different stress ranges. It can be seen that for higher values of N_f the increase in crack width at same number of cycles becomes less significant. For example, if $N_f = 6 \times 10^6$ cycles, the increase in crack width at 600,000 cycles is only about 18% while if $N_f = 667,000$ cycles the increase in crack width is about 449%. This observation can be beneficially used in design to reduce the effect of fatigue on crack widths.

CONCLUSION

The subject of cracking is a complex one for both reinforced concrete and ferrocement; exhaustive experimental investigations combined with scrupulous analysis are still necessary in ferrocement to better ascertain the influence of major parameters and separate their effects. The above study is based on experimental tests of ferrocement specimens reinforced mostly with square meshes of relatively small sizes and represents in a way the present state of knowledge. Similar studies exploring different types of reinforcement (such as expanded metal, chicken wire meshes, a combination of mesh and rod-type reinforcement) and a wider range of sizes are needed before generalizing some of the above derived results.

ACKNOWLEDGEMENT

This study was made possible by a grant (ENG 74-20829) from the National Science Foundation (Engineering Mechanics Section, Structural Materials and Geotechnical Engineering Program) to the University of Illinois at Chicago Circle, Department of Materials Engineering.

REFERENCES

1. Rilem, Proceedings of the Symposium on Bond and Crack Formation in Reinforced Concrete, Stockholm, Sweden, 1957.
2. Ferry, Borges, J., "Cracking and Deformability of Reinforced Concrete Beams," International Association for Bridge and Structural Engineering, Vol. 26, Zurich, 1966, pp. 75-95.

3. "Causes, Mechanism and Control of Cracking in Concrete," American Concrete Institute Special Publication SP20, Detroit, Michigan, July 1968.
4. Gergely, P. and Lutz, L. A., "Maximum Crack Width in Reinforced Concrete Flexural Members," American Concrete Institute, Publication SP20, Detroit, Michigan, 1968, pp. 87-117.
5. Atlas, S., Siess, C. B. and Kesler, C. E., "Control of Cracking in Slabs Reinforced with Welded Wire Fabric," American Concrete Institute, Publication SP20, 1968, pp. 205-209.
6. Nawy, E. G. and Huang, P. T., "Crack and Deflection Control of Pretensioned Prestressed Beams," Journal of the Prestressed Concrete Institute, Vol. 22, No. 3, May/June 1977, pp. 30-47.
7. "Control of Cracking in Concrete Structures," ACI Committee 224, Journal of the American Concrete Institute, Vol. 69, No. 12, Dec. 1972, pp. 717-753.
8. Proceedings of the American Concrete Institute Symposium on "Practical Control of Cracking in Concrete Structures," Annual Convention, New Orleans, Louisiana, Oct. 1977.
9. Shah, S. P. and Naaman, A. E., "Crack Control in Ferrocement and Its Comparison with Reinforced Concrete," Presented at the ACI Symposium on "Practical Control of Cracking in Concrete Structures," New Orleans, Louisiana, Oct. 1977.
10. Balaguru, P. N., Naaman, A. E. and Shah, S. P., "Analysis and Behavior of Ferrocement in Flexure," ASCE Journal of the Structural Division, Vol. 103, No. ST10, Oct. 1977, pp. 1937-1951.
11. Balaguru, P. N., Naaman, A. E. and Shah, S. P., "Ferrocement in Bending, Part I: Static Nonlinear Analysis," Dept. of Materials Engrg., Univ. of Ill. at Chicago Circle, Report No. 76-2, Aug. 1976, 144 pp., NTIS #PB-262155/AS.
12. Balaguru, P. N., Naaman, A. E. and Shah, S. P., "Ferrocement in Bending, Part II: Fatigue Analysis," Department of Materials Engineering, Univ. of Ill. at Chicago Circle, Report No. 77-1, Oct. 1977, 246 pp.
13. Naaman, A. E. and Shah, S. P., "Tensile Tests of Ferrocement," Journal of the American Concrete Institute, Vol. 68, No. 9, Sept. 1971, pp. 693-698.
14. Somayaji, S., Shah, S. P. and Naaman, A. E., "Tensile Cracking and Stress Strain Curve of Ferrocement, Part I: Effect of Longitudinal Reinforcement," Dept. of Materials Engrg., Univ. of Ill. at Chicago Circle, Report in Progress.

Crack Width Prediction

37

15. Guerra, A. J., Naaman, A. E. and Shah, S. P., "Ferrocement Cylindrical Tanks: Cracking and Leakage Behavior," Journal of the American Concrete Institute, Vol. 75, No. 1, Jan. 1978, pp. 22-30.
16. Guerra, A. J., Naaman, A. E. and Shah, S. P., "Cracking and Leakage Characteristics of Ferrocement Water Tanks," Dept. of Materials Engrg., Univ. of Ill. at Chicago Circle, Report #76-3, Sept. 1976, 54 pp., NTIS #PB 258003/RC.

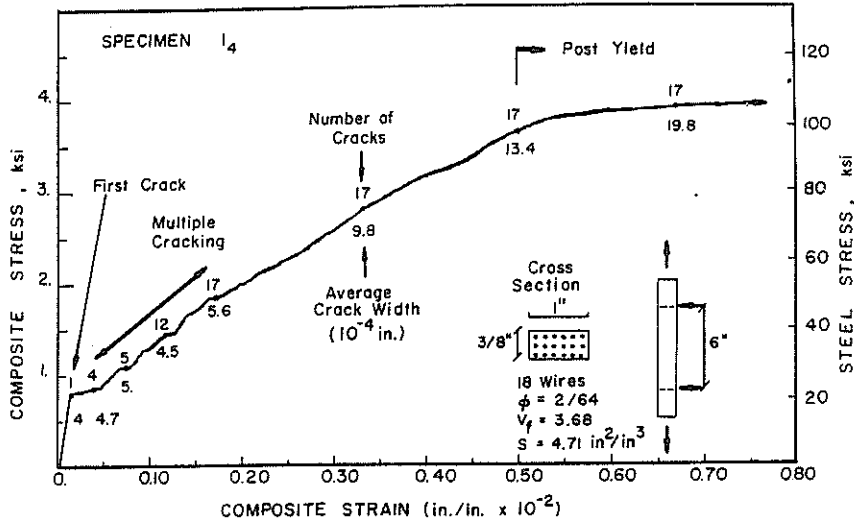


Fig. 1 Typical stress-strain curve in tension of composite without transverse reinforcement.

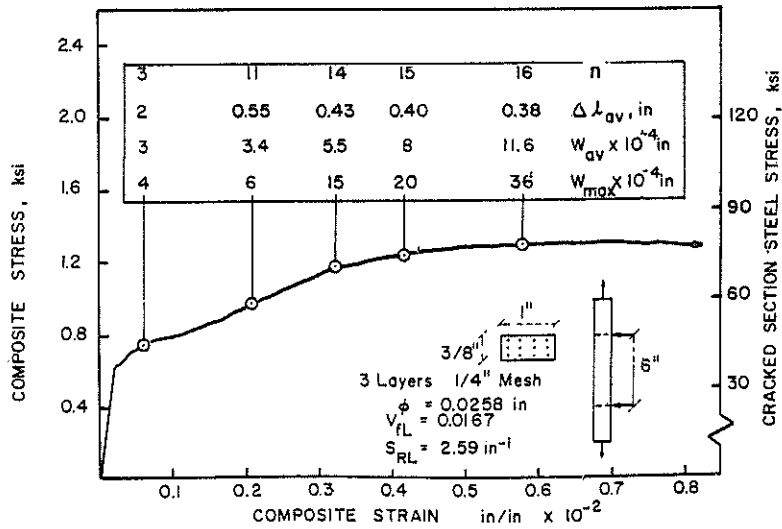


Fig. 2 Typical stress-strain curve in tension of composite reinforced with square meshes.

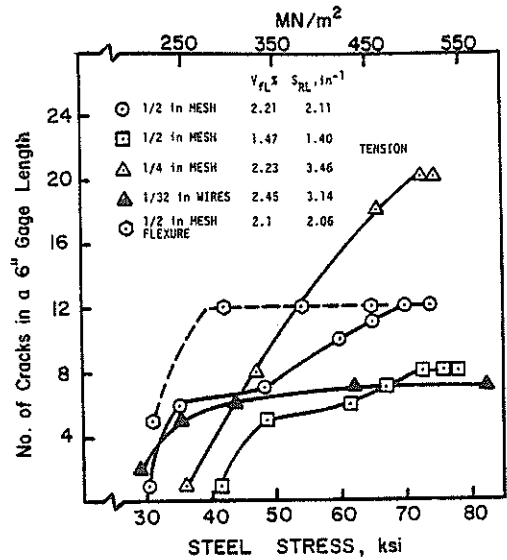


Fig. 3 Typical crack development with steel stress for tensile and flexural specimens.

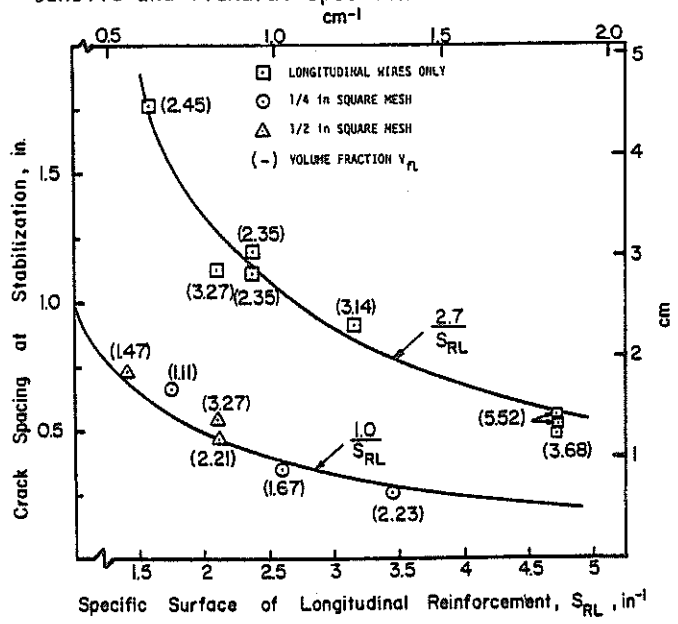


Fig. 4 Variation in crack spacing at crack stabilization with the specific surface of reinforcement.

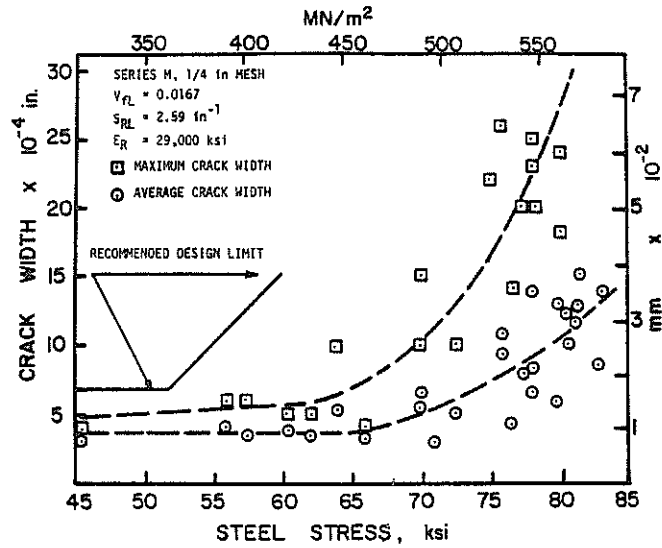


Fig. 5 Typical variations of crack widths in tension versus steel stress.

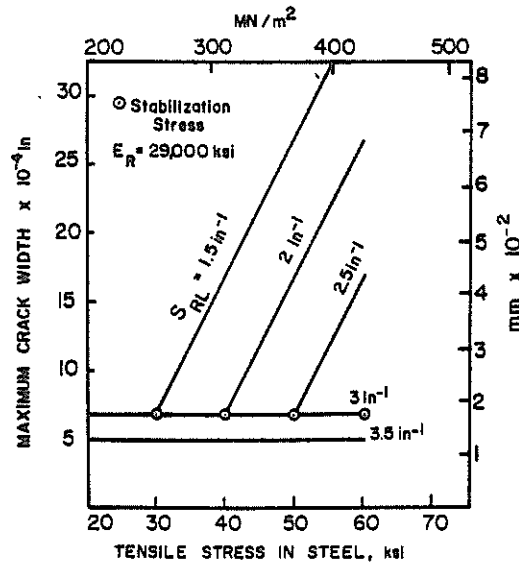


Fig. 6 Proposed maximum crack width prediction in tension for ferrocement reinforced with square meshes.

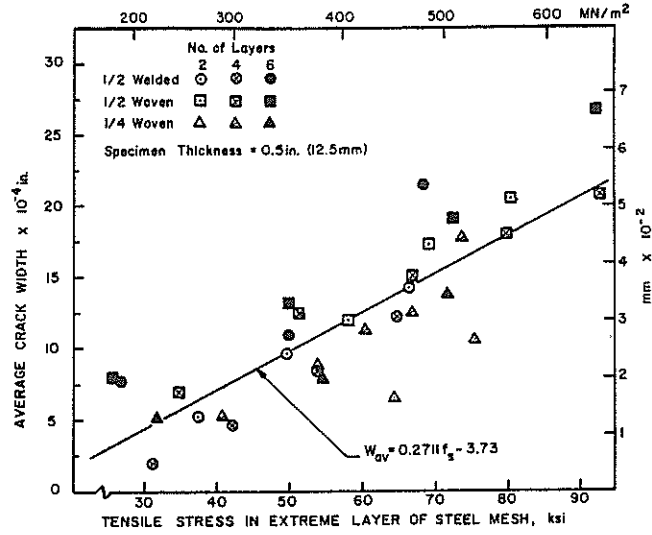


Fig. 7 Observed variation of average crack width in flexure versus steel stress.

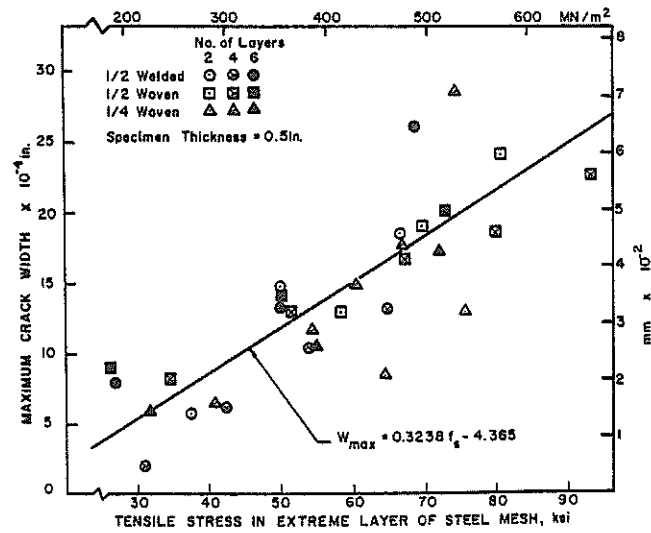


Fig. 8 Observed variation of maximum crack width in flexure versus steel stress.

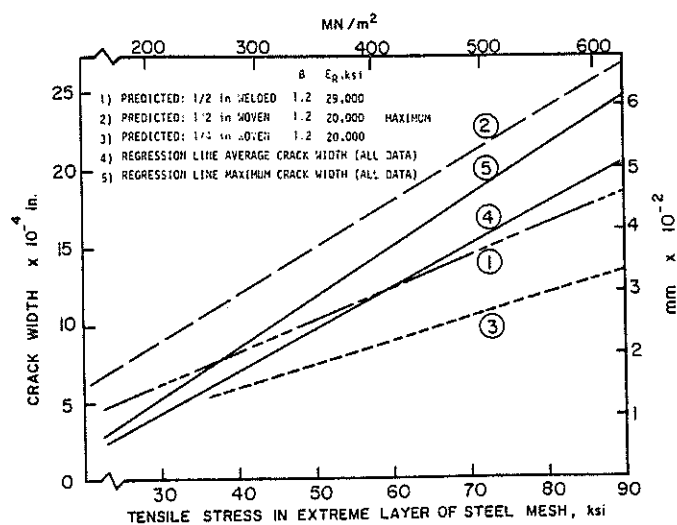


Fig. 9 Comparison of predicted and observed crack widths in flexure.

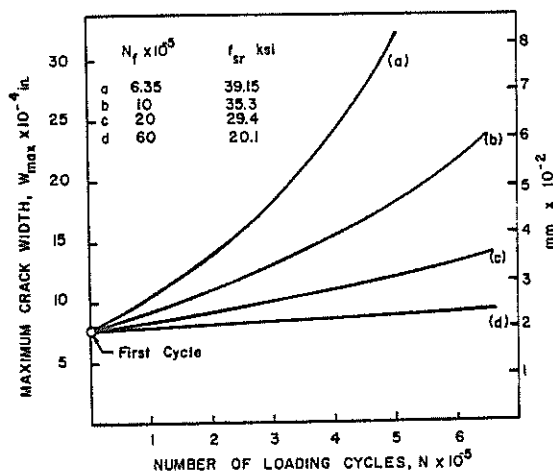


Fig. 10 Typical crack width increase with loading cycles.